Journal of Polymers and the Environment
https://doi.org/10.1007/s10924-020-01925-2

ORIGINAL PAPER

Carbamoylethylated Wood Pulp as a New Sorbent for Removal of Hg (II) from Contaminated Water: Isotherm and Kinetic Studies

A. Hashem[1] · A. J. Fletcher[2] · A. Safri[2] · A. Ghith[3] · D. M. Hussein[3]

Accepted: 7 October 2020

Abstract

Mercury is a persistent, heavy metal present in watercourses, and this paper presents the synthesis of a new, low-cost sorbent, based on wood pulp, for the targeted removal of Hg (II) from aqueous solutions. Carbamoylethylated wood pulp sorbents were obtained from the reaction of wood pulp with acrylamide, in basic media, to produce a suite of materials with varying nitrogen concentration (0.251.51%). Batch sorption techniques were used to determine the sorption capacity of each sorbent for Hg (II), as a function of pH, contact time, as well as sorbate and sorbent concentrations. The samples were evaluated for bulk and surface chemistry (nitrogen concentration and FTIR) as well as surface morphology and textural properties (SEM and surface area measurements). Sorption analysis via Langmuir, Freundlich and Temkin models, showed that the data were best represented by the Temkin isotherm model suggesting influence from surface heterogeneity in the adsorption process. Langmuir analysis provides an indication of the maximum sorption uptake at 787.6 mg g^{-1}, while Freundlich analysis shows the sorption process to be favourable but with some slight suppression at low concentrations. The results indicate the importance of nitrogen concentration and corresponding sorption capacity in Hg (II) sorption kinetics and are consistent with the recovery rates observed. Sorption tests demonstrate that these sorbents have remarkable potential, which is validated through 39% removal of Hg (II) from aqueous solution, and modelling of the kinetic data showed that the system closely flows a pseudo-second-order kinetic model.

Keywords Sorption · Mercury (II) ions · Carbamoylethylation · Kinetics · Isotherms

Introduction

Mercury is one of the most toxic heavy metals present in effluents generated by commercial and industrial activities. Although mercury has significant uses in the energy, chemicals, metallurgy, electronics, and alkali industries [1], its industrial usage has been impacted due to environmental concerns [1]. Unlike other organic contaminants, mercury cannot be biologically degraded and therefore, is identified as a potential health concern. The maximum mercury concentration recommended by the World Health Organization is 0.001 ppm [2]. It has been found that mercury has a tendency to convert into highly toxic compounds that are hazardous to the human body [3]. These compounds, or mercury in any form, affects the kidneys and can cause renal failure, acute gastrointestinal damage, or cardiovascular collapse [4]. Additionally, the ingestion of mercury-contaminated drinking water is a potential threat to foetal development [5]. Hence, the removal of mercury from water systems becomes essential and, therefore, has attracted significant attention in recent years.

Conventional methods for the removal of mercury include ion exchange, chemical precipitation, reverse osmosis, electrodialysis, as well as sorption by activated carbon or natural materials [6]. Amongst these methods, sorption appears to be the simplest and least challenging [7]. Adsorption is one of interest to many economic sectors and concerns areas such as food and pharmaceutical industries, chemistry, and the treatment of industrial wastewater.

Generally, sorption capacity depends on several factors such as the type of sorbent, operating conditions, targeted

✉ A. J. Fletcher
ashleigh.fletcher@strath.ac.uk

[1] National Research Center, Textile Research Division, Dokki, Cairo, Egypt

[2] Department of Chemical and Process Engineering, University of Strathclyde, 75 Montrose Street, Glasgow G1 1XJ, UK

[3] Chemistry Department, Faculty of Science, Sebha University, Sebha, Libya

Published online: 18 October 2020

pollutants, regeneration and reusability [8], and previous studies have reported activated carbon as a sorbent for the removal of mercury [9]. However, regeneration cost makes it difficult to be put into practice in developing countries where such measures are needed, therefore, there is a need for suitable alternative sorbents for use in water treatment.

More recently, agricultural wastes, as sorbents, have been investigated widely for heavy metal sorption [7]. The use of these sorbents is of interest due to the low-cost processing, ease of availability of free resources, and favourable physicochemical properties. In order to increase both metal sorption capacity and efficiency, the pre-treatment of these agricultural wastes may be needed. For example, chemically modifying these sorbents can increase the sorption capacity, which may be achieved via modification of the backbone of cellulosic materials through functionalisation of the pre-existing hydroxyl groups, which has been shown to enhance the sorption capacity of metal ions [1, 10–12].

Based on this rationale, the work presented here focusses on the production of carbamoylethylated wood pulp (CEWP) for the enhanced sorption of mercury ions from aqueous solution. The effect of altering reaction conditions in the carbamoylethylation step, such as contact time, pH, and sorbent and sorbate concentrations, on the sorptive capacity of the modified wood pulp was investigated. The sorption data were analysed using Langmuir, Freundlich and Temkin models at 30 °C using non-linear regression analysis to determine the best sorption kinetics and isotherm models for mercury sorption onto CEWP.

Experimental

Materials and Reagents

The wood pulp (WP) used in this study was supplied by Rakta Company, Alexandria, Egypt. The reagents, mercuric acetate, sodium hydroxide, ethylenediaminetetraacetic acid (EDTA), nitric acid, sodium carbonate, hydrochloric acid, acetone, and ethyl alcohol, were all laboratory grade chemicals procured from Merck, Germany.

Preparation of Carbamoylethylated Wood Pulp (CEWP)

Four sorbent samples of CEWP were prepared through carbamoylethylation of WP, as represented in Table 1. The amount of acrylamide was varied as other reaction conditions were kept constant. 4 g of wood pulp was mixed with a specific volume and known concentration of sodium hydroxide. Acrylamide, dissolved in a minimum amount of distilled water, was added to the mixture and mechanically stirred to form a homogenous paste that was transferred to Erlenmeyer flask and placed in a water bath shaker at 60 °C for 2 h; following which the samples were left to cool at room temperature. The resulting samples were washed with a mixture of water and ethanol (20:80) in order to remove excess alkali, unreacted acrylamide, and soluble by-products. In this investigation, the sorbent with the highest nitrogen content (1.51%) was selected for sorption of Hg (II) ions.

Table 1 The Samples of CEWP Prepared in this Study and their Sorption Performance

Nitrogen %	Adsorption Capacity, qe(mg/g)	% Removal
0.25	53.2	4.3
0.53	106.4	8.7
0.84	266.1	21.7
1.51	479.0	39.1

Reaction conditions: Wood pulp, 4 g; NaOH, 30 mmol; acrylamide (7–60 mmol); reaction temperature, 60 °C and reaction time, 2 h

Sorbent Characterization

Fourier-Transform Infrared Spectroscopy (FT-IR)

The FT-IR spectroscopy was used to determine the functional moieties on the surface of the WP, CEWP, and CEWP loaded with Hg (II), and also to determine the chemical linkages present between the surface of the sorbent and the sorbate. The FT-IR spectra of the samples were recorded on KBr discs containing 2–10 mg of sample in 300 mg of KBr, and recorded using a Perkin–Elmer Spectrum 1000 spectrophotometer over a wavelength range of 4000–400 cm^{-1} at a scanning interval of 1 cm^{-1} over 120 scans.

Scanning Electron Microscopy (SEM)

Morphological analysis of sorbent samples, coated with chromium prior to analysis, were performed using a scanning electron microscope (SEM) (TESCAN CE; Type: VEGA 3 SBU; No.:117–0195- Czech Republic). Images of sample morphology were recorded at 2000 × magnification.

Energy–Dispersive X-ray Analysis (EDX)

The energy-dispersive X-ray pattern (EDX) of the CEWP sample was recorded by use of a dispersive X-ray fluorescence (EDX) spectrometer (Oxford Instruments) attached to an SEM Model JEOL-JSM-5600. The test was performed only after sorption to examine the presence or absence of mercury metal through its characteristic band.

BET Surface Area Analysis

The surface area measurement of each sorbent were investigated by employing nitrogen sorption on an Autosorb I at −196 °C and applying Brunauer-Emmet-Teller theory to the resulting data. The mesopore volume, external surface area, and mesopore surface area were determined using the t-plot method, while the Barrett-Joyner-Halenda technique was used to calculate the average pore width and determine the pore size distribution.

A solid addition method was used to characterize the surface chemistry of CEWP by evaluating the pH of the sorbent at the point of zero charge (pH_{PZC}). Typically, 100 mL of 0.01 N NaCl was added to a series of conical flasks and the pH adjusted using an aqueous solution of 0.01 N HCl or 0.01 N NaOH, respectively, in the range of 2 to 12. The initial pH was recorded after a constant value was attained. Thereafter, an accurate mass of 100 mg of CEWP was dispersed in each conical flask and incubated for 24 h to obtain the final pH. The initial and final pH were plotted, where the intersection points of the plots were denoted as the pH_{PZC} of the sorbent.

The nitrogen content of carbamoylethylated wood pulp samples was determined using the micro-Kjeldahl method [13].

Batch Sorption Studies

0.03 g of the sorbent was added to 100 mL of a Hg (II) ion solution (100–1000 mg L^{-1}). The pH value of the mixture was adjusted, according to the pH_{PZC}, by dropwise addition of 0.1 M HNO_3 or 0.1 M NaOH and the mixture shaken at a constant speed (150 rpm) at 30 °C for a predefined period. The final metal ion solution was filtered and the concentration of Hg (II) ions measured before and after sorption, using direct titration with a standard EDTA solution (0.5 mM).

The amount of Hg (II) sorbed at equilibrium, q_e (mg g^{-1}), was calculated using Eq. 1, while the percentage removal was calculated via Eq. 2.

$$q_e = \frac{V(C_o - C_e)}{W} \tag{1}$$

$$\text{Removal } \% = \frac{(C_o - C_e)}{C_o}.100 \tag{2}$$

where C_o and C_e (mg L^{-1}) are the initial metal concentration and metal concentration at equilibrium, respectively; W (g) is the weight of sorbent used, and V is the volume of Hg (II) solution (0.1 L).

Error Analysis

The adequacy and integrity of the obtained kinetic models and isotherm models applied over the experimental data ranges were evaluated using the coefficient of determination (R^2) and absolute relative error (ARE) [14], as expressed in Eqs. 3 and 4, respectively. Minimum ARE and R^2 values approaching unity were used as criteria for selection of the kinetic and isotherm models that best described the experimental data.

$$R^2 = \frac{\sum (q_{ecal} - q_{mexp})^2}{\sum (q_{ecal} - q_{mexp})^2 + (q_{ecal} - q_{mexp})^2} \tag{3}$$

$$ARE = \frac{100}{n} \sum_{i=1}^{n} \left[\frac{q_{e,i,cal} - q_{e,i,exp}}{q_{e,i,exp}} \right] \tag{4}$$

where n, q_{exp}, and q_{cal} are the range of input data, experimental, and calculated uptake of Hg (II) ions, respectively.

Results and Discussion

Sorbent Characterization

FTIR Analysis

The FT-IR spectra for WP, CEWP and CEWP loaded-Hg (II) are illustrated in (Fig. 1a-c), respectively. The difference in the fingerprint peaks of the spectra are clear and confirm the carbamoylethylation and sorption processes. The spectra of native WP (Fig. 1a) show a band at 3334 cm^{-1}, characteristic of O–H stretching. The sharp peak at 2918 cm^{-1} is attributed to backbone C-H stretching, while the band at 1685 cm^{-1} is attributed to C=O stretching. Finally, the peak at 1057 cm^{-1}

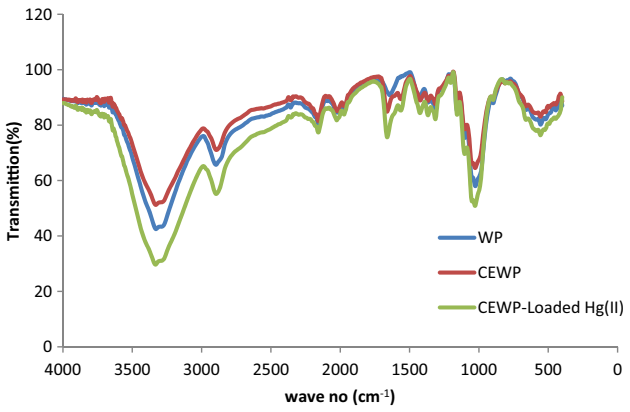

Fig. 1 FT-IR of (a) wood pulp (WP); (b) carbamoylethylated WP (CEWP), and (c) CEWP-loaded-with Hg (II) ions

is due to the C-O stretching of primary alcohols, which symbolizes the glucose ring, and the intensity of this peak was unchanged after modification. (Fig. 1b) exhibits broadness at 3350 cm^{-1} due to hydrogen bonding between the –OH group of WP and amine groups in the chains of CEWP. The peak at 2916 cm^{-1} is attributed to C-H stretching and the peak at 1059 cm^{-1} is due to C-H bending. This demonstrates the successful modification of WP via carbamoylethylation.

(Fig. 1c) shows a small shift in the absorbance peaks in Hg (II)-loaded CEWP compared with that in WP (Fig. 1a) and CEWP (Fig. 1b), indicating the strengthening of relevant bonds. The broad band observed at 3350 cm^{-1} shifts to 3363 cm^{-1}; 2916 and 2192 cm^{-1} shift to 2925 and 2185 cm^{-1}, respectively; while the peaks previously observed at 1675 and 1059 cm^{-1} were shifted to 1672 and 1061 cm^{-1}, respectively, which can be attributed to the adsorption of Hg (II)ions onto CEWP.

Morphological Analysis

Surface morphologies of the CEWP, and Hg (II)-loaded CEWP samples are shown in (Fig. 2a, b), respectively. SEM reveals the irregular nature of the particles, which are rough and heterogeneous with a considerable amount of void

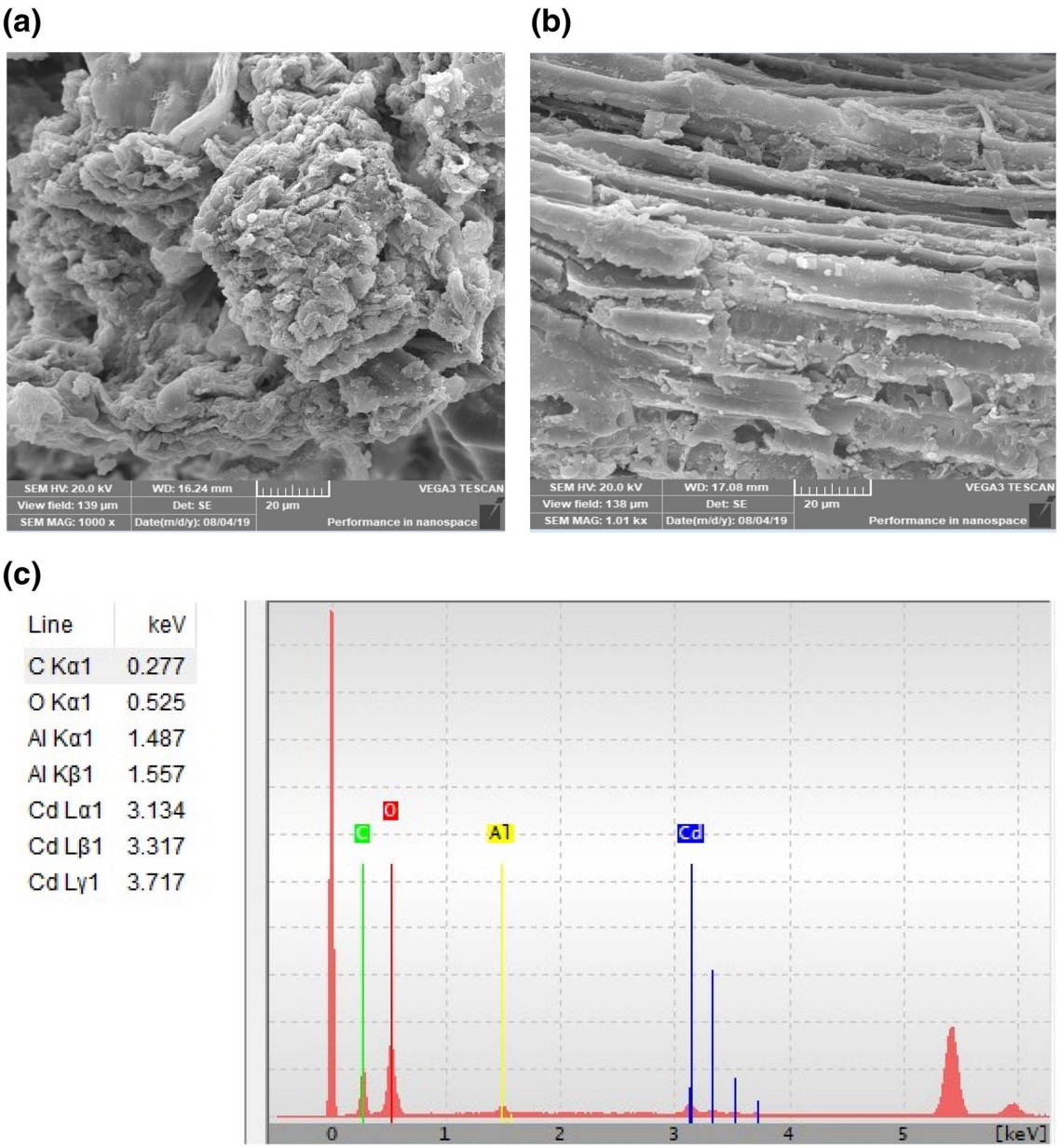

Fig. 2 SEM of **a** carbamoylethylated wood pulp (CEWP), **b** CEWP-loaded Hg (II) ions, and **c** EDX of CEWP loaded with Hg (II) ions

space. After Hg sorption, the cavities appear to be prominently swollen as Hg enters the pores of CEWP (Fig. 2b). This observation indicates that Hg is sorbed onto the rough and heterogeneous points present in the CEWP structure suggesting that the sorbent can be used for liquid–solid sorption processes.

The EDX spectra of Hg (II)-loaded CEWP is presented within the chart of Fig. 2c. The presence of sharp peaks corresponding to Hg element in the Hg (II)-loaded CEWP sample affirmed adsorption of Hg (II) onto CEWP surface.

Textural Characterisation

The textural characteristics of CEWP, as determined from nitrogen sorption analysis, show a very low BET surface area of 8 $m^2\ g^{-1}$ with a total pore volume of 0.018 $cm^3\ g^{-1}$ and an average pore width of 9 nm. The low BET surface area is expected due to the nature of the WP and its conversion to CEWP. The average pore width is in the mesopore region, which is beneficial for mass transport and sorption of Hg (II). Hence, the high sorption capacity of CEWP is independent of the surface area and could be related to the high density of active surface functional groups. Similar studies on relatively high metal sorption on low specific surface area sorbents have been reported in the literature [15, 16].

Factors Affecting Sorption of Hg (II)

Several factors influencing the sorption process of heavy metals, such as pH, sorptive concentration, sorbent dose, and contact time, were investigated to understand their impact on the sorption behaviour of CEWP.

Point of Zero Charges (pH_{PZC}) and the Effect of pH

Fig. 3 shows the data obtained for pH_{PZC} determination for the surface of the CEWP sorbent, allowing the pH at which the surface of CEWP has a neutral charge to be determined.

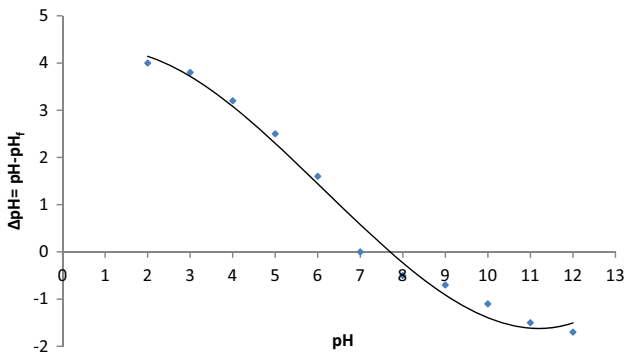

Fig. 3 pH of point of zero charge of onto carbamoylethylated wood pulp (CEWP)

The pH_{PZC} of CEWP can be observed to be 7.0, indicating that the surface of CEWP is neutral in nature. When the pH value of the solution is higher than pH_{PZC}, the surface charge of sorbent will be negative and favours the binding of cations. When the pH value of the solution is lower than the pH_{PZC}, the surface charge of a sorbent will be positive and therefore, the sorption of cations is not favourable [17].

The results of studies into the effect of pH on the sorption of Hg (II) ions by CEWP, in the range pH 2–6, and an initial mercury ion concentration of 300 mg L^{-1}, is shown in Fig. 4. The sorption of Hg (II) increased from 0 to 85.1 mg g^{-1} with increasing pH, up to 5, and then decreased with a further increase of pH within the range studied. At high acidity (pH 2), the CEWP surface will be completely covered with H_3O^+ ions, and Hg (II) ions would be able to compete with them for sorption sites ($q_e = 45.1$ mg g^{-1}). With the increase in pH, the competing effect of H_3O^+ decreases and the positively charged Hg (II) ions would sorb on the free binding sites of the sorbents indicating a maximum value at pH 5. After this point, the uptake decreases again, as active sites are less available on the sorbent, and equilibrium is established between the mercury ions on the sorbent and in solution. The.pH values higher than 6 results in the precipitation of Hg ions [1]. Thus, the pH was kept below 6 in all runs.

Similar results were reported in literature with another adsorbent confirming the important role of pH in Hg binding process [18].

The optimum pH observed here is lower than the pH_{PZC}, and leads to the sorbent surface being predominantly positive, which may lead to electrostatic repulsion between the Hg (II) ions and positively charged surface [19]. The positively charged surface of the CEWP can be attributed to the protonation behaviour of the nitrogen atoms in the $-NH_2$ groups introduced onto the surface of WP as a result of the reaction with acrylamide. The sorption mechanism for mercury ions can be attributed to the formation of metal

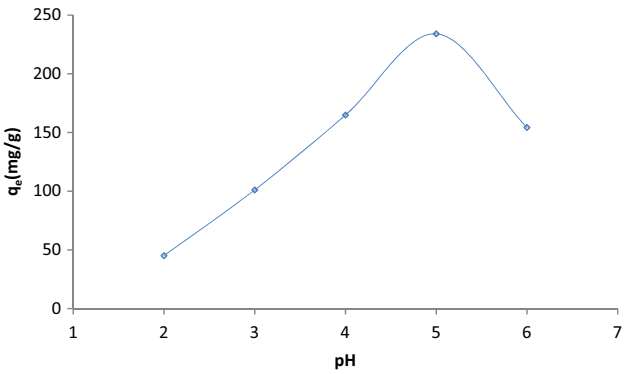

Fig. 4 Effect of pH on adsorption capacity of Hg (II) ions onto carbamoylethylated wood pulp (CEWP) (reaction conditions: mercury acetate concentration: 300 mg/L; adsorbent concentration: 0.3 g/L; contact time: 1 h; reaction temperature: 30 °C)

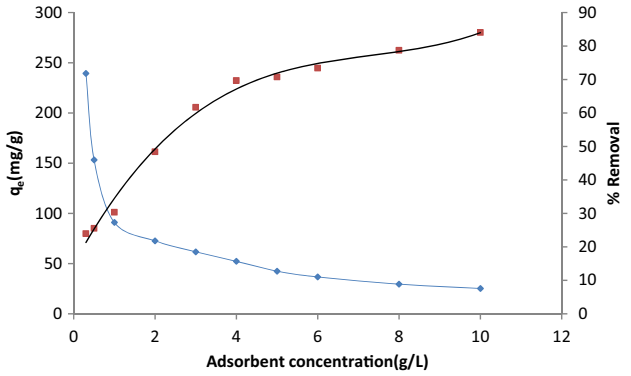

Fig. 5 Effect of adsorbent concentration on adsorption capacity (diamond) and percentage removal (square) of Hg (II) ions onto carbamoylethylated wood pulp (CEWP)(reaction conditions: mercury acetate concentration: 300 mg/L; pH 5; contact time: 1 h; reaction temperature: 303 K)

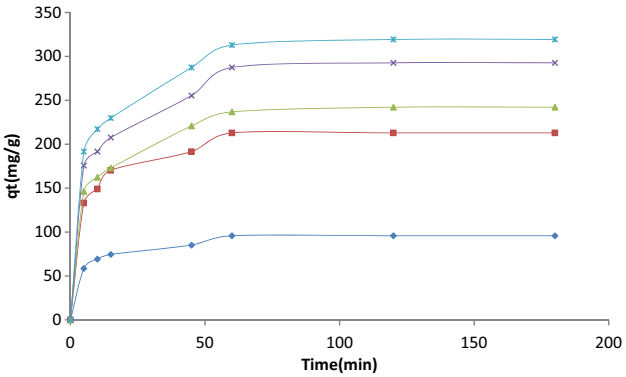

Fig. 6 Effect of contact time and adsorbate concentration on adsorption capacity of Hg (II) ions onto carbamoylethylatedwood pulp (CEWP) using different concentrations of mercury acetate solution (diamond 100 mg/L; square 200 mg/L; triangle 300 mg/L; cross 600 mg/L; star 700 mg/L).Reaction conditions: mercury acetate concentration: 300 mg/L; pH 5; contact time: 1 h; reaction temperature: 30 °C

complexes with the nitrogen in the amine groups of the CEWP. For mercury ion removal, the formation of metal complexes with both the nitrogen atoms in the amine groups and the oxygen atoms in CEWP may play an important role.

Effect of Sorbent Dose

It has been previously observed, that sorbent dose influences the uptake of target species from solution, including metal ions. The effect of sorbent dose on the sorption capacity of CEWP for Hg (II) ions was studied at the previously determined optimum pH of 5, using sorbent doses in the range 0.3–10 g L^{-1}, and an initial metal ion concentration of 300 mg L^{-1} (Fig. 5). It can be seen that the sorption capacity (q_e) of Hg (II) ions, per gram of sorbent (mg g^{-1}), decreased from 239.8 to 23.2 mg g^{-1} with increasing sorbent dose up to 8 g L^{-1}, where after steady-state is observed. The decrease in sorption capacity with increasing sorbent dose can be attributed to the high number of unsaturated sorption sites, hence, a relative decrease per unit mass, as well as overlapping of sorption sites, and overcrowding of the sorbent particles, as has been observed previously for Zn(II) [20]. It should also be noted that the percentage removal of Hg (II) ions onto CEWP increased with increasing sorbent concentration, which may be due to the increase in the surface area of the sorbent. Thus, 0.3 g/L can be adopted as the best dose value which gives highest adsorption capacity for Hg ions which is in accordance with similar study in the literature [1].

Effect of Contact Time

Fig. 6 shows the effect of agitation time on the sorption capacity of Hg (II) onto CEWP using initial concentrations of 100, 200, 300, 600 and 700 mg L^{-1}, at fixed sorbent concentration and fixed temperature (30 °C). The amount of Hg (II) sorbed (mg g^{-1}) increases with increasing agitation time, and reached equilibrium after 60 min for all Hg (II) concentrations used in this study.

This equilibrium time is relatively short [21], which is an important consideration in the development of an economically viable wastewater treatment system. The reported saturation at 60 min for Hg adsorption on CEWP is lower than 120 min which was reported on Ziziphus spina-christi L [18]. It is clear that the sorption capacity depends on the concentration of the Hg (II) ions, with all sorption curves exhibiting monolayer formation through continuous sorption leading to saturation.

Isothermal Analysis of Hg (II) Ion Sorption on CEWP

A sorption isotherm describes the thermodynamic equilibrium established between the amount sorbed on the sorbent surface with the amount of sorptive remaining in solution. Several models have been developed to describe the behaviour that may be observed in sorption systems, and a range of those based on two parameters was used to analyse the data obtained in this study, these are Langmuir, Temkin, and Freundlich. All isothermal data analysed was obtained for sorption of Hg (II) ions onto 0.3 g L^{-1} of CEWP, at pH 5 and 30 °C, allowing an equilibration time of 60 min.

The Langmuir Equation [22] is based on monolayer sorption with a fixed number of localised sites; the model refers to homogeneous sorption, meaning that the sorption activation energy and the enthalpies evolved by each sorbate molecule are equal, also, there are no interactions between neighbouring sorbate molecules, nor any site to site

movement of sorbed species. The non-linear form of the Langmuir isotherm is:

$$q_e = \frac{K_L C_e}{1 + bC_e} \tag{5}$$

where C_e is the concentration of Hg (II) ions sorbed at equilibrium, mg L^{-1}, q_e is the amount of Hg (II) ions sorbed per unit mass of sorbent (mg g^{-1}), K_L (L g^{-1}) and b (L mg^{-1}) are constants, and the ratio b/k_L gives the maximum sorption capacity (q_{max}) in mg g^{-1}.

The Freundlich isotherm can be applied to systems that exhibit multilayer sorption, mathematically predicting infinite surface coverage at high sorptive concentrations, and accounts for surface heterogeneity, where the strongest binding sites are occupied first, and the total amount sorbed is the cumulative sorption across all surface sites. The decrease in heats of sorption across all surface sites is assumed to be logarithmic, and the logarithmic form of the model is [23]:

$$q_e = K_F . C_e^{1/n} \tag{6}$$

where C_e and q_e are as defined above, and K_F and n are constants related to the sorption capacity and favourability, respectively.

By contrast, the Temkin isotherm model [24] assumes that there is a linear decrease in the distribution of heats of sorption across all surface sites due to sorbate/sorbent interactions, rather than the logarithmic trend assumed in the Freundlich model. The non-linear Temkin isotherm model is represented by:

$$q_e = \frac{RT}{b_T} . ln\left(A_T C_e\right) \tag{7}$$

where C_e and q_e are as defined above, A_T is the Temkin isotherm constant (L g^{-1}), b_T is a constant related to the heat of sorption (J mol^{-1}), T is the absolute temperature (K), and R is the universal gas constant(8.314 J mol^{-1} K^{-1}).

Error Analysis

To determine the most accurate model of the isothermal data obtained in this study, the error distribution between the experimental data and the data derived from predicted isotherm models was minimised using error functions. The experimental isotherm data obtained in this study were analysed using three isotherm models, i.e. Langmuir, Freundlich, and Temkin. Errors between experimental and isothermal model data were minimized using the error function of ARE which were optimised using non-linear regression. Fig. 7 shows a comparison between the experimental isothermal data obtained in this study and the theoretical fits

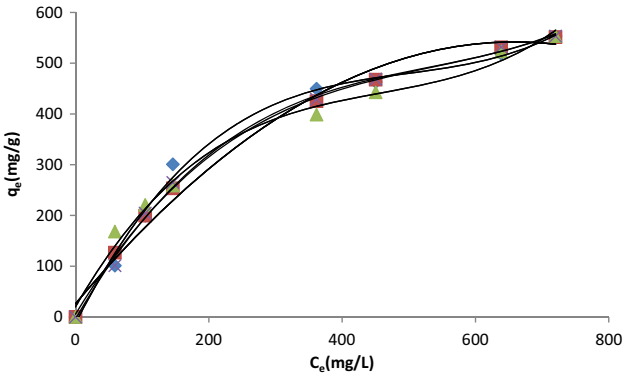

Fig. 7 Equilibrium experimental adsorption data obtained for Hg (II) ions onto carbamoylethylatedwood pulp (CEWP) at 30 °C (blue), and resulting fits from Langmuir (red), Freundlich (green) and Temkin models (yellow).Reaction conditions: mercury acetate concentration: 300 mg/L; pH 5; contact time: 2 h; reaction temperature: 30 °C

Table 2 Isotherm Constants for Hg (II) Ions Adsorption onto CEWP at 30 °C

Isotherm Model	Parameter	Value	Error Analysis	Value
Langmuir	a_L	0.0033 L mg^{-1}	R^2	0.9968
	q_{max}	787.6 mg g^{-1}	ARE	0.5022
	k_L	2.56L g^{-1}		
Freundlich	n	2.10	R^2	0.9912
	K_F	24.07 mg g^{-1}	ARE	1.0728
Temkin	A_T	0.0296	R^2	0.9983
	b_T	13.92	ARE	0.2271

offered by Langmuir, Freundlich and Temkin. Additionally, Table 2 presents the R^2 and ARE for the isotherm models used. Langmuir analysis provides a good level of fit, and also allows the maximum adsorption capacity to be determined; this is found to be 787.6 mg L^{-1} for Hg (II) ions onto CEWP. The value of n obtained from the Freundlich model (Table 2), again showing a reasonable level of fit, was 2.1, satisfying $0 < n < 10$, which also indicates that sorption of Hg (II) ions onto CEWP is favourable. The value of $1/n < 1$ suggests a slight suppression of sorption at lower equilibrium concentrations. Overall, Table 2 shows that the isotherm models are ordered, in terms of best fit to the experimental data, as Temkin > Langmuir > Freundlich. This suggests that the adsorption behaviour is influenced by a heterogenic character from the sorbent, as also shown from the SEM analysis.

In comparison with other adsorbents reported in the literature for adsorption of mercury, the CEWP adsorbent offers a high degree of affinity for removal of mercury, as shown in Table 3 [1, 18, 25–29].

Table 3 Comparison of Adsorption Capacities of Various Adsorbents Towards Hg (II)

Adsorbent	Adsorption Capacity (mg/g)	References
Phosphorylated haloxylon ammodendron	416.7	1
P. turgidum roots	333.33	25
Ziziphus spina-christi L	37.45	18
Aminated hydroximoyl camelthorn residues (AHCR)	272.9	26
Functionalized bagasse-derived carbon	98	27
Thiosemicarbazide-modified cellulose	331.1	28
Chemical-modified peanut hull	83.3	29
Carmamoylethylated wood pulp (CEWP)	687.6	Present study

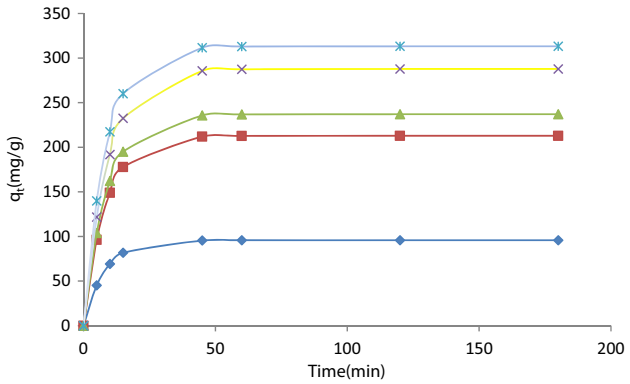

Fig. 8 Non-linear plots of pseudo-first-order models for adsorption of Hg (II) ions onto carbamoylethylatedwood pulp (CEWP) at different concentrations (diamond 100 mg/L; square 200 mg/L; triangle 300 mg/L; cross 600 mg/L; star 700 mg/L).Reaction conditions: mercury acetate concentration: 300 mg/L; pH 5; contact time: 1 h; reaction temperature: 30 °C

Sorption Kinetics

In addition to studying the equilibrium behaviour of sorption systems, it is critical to understand their approach to this equilibrium by also studying the kinetics of sorption, which can provide insight into the mechanism of sorption. In this work, three models were used to represent the kinetics of Hg (II) sorption onto CEWP: pseudo-first-order, pseudo-second-order and intra-particle diffusion. The kinetic process of the pseudo-first-order is usually considered physical sorption and is diffusion controlled. The non-linear mathematical form of the pseudo-first-order model [30] is given by:

$$q_t = q_e\left[1 - \exp\left(-k_1 t\right)\right] \tag{8}$$

where q_t is the amount of Hg (II) ions sorbed (mg g^{-1}) at time t (min), q_e is the amount of Hg (II) ions sorbed (mg g^{-1}) at equilibrium, and k_1 is the rate constant of sorption (min^{-1}). The non-linear plots of pseudo first-order of Hg (II) ions onto CEWP at concentrations of 100, 200, 300, 600 and 700 mg L are shown in Fig. 8. The values of k_1, and q_e along with R^2, and ARE were summarized in Table 4. The pseudo-second order kinetic model [31] can be expressed by:

Table 4 Kinetic Parameters for the Adsorption of Hg (II) Ions onto CEWPat Different Initial Concentrations

Parameters	C_o(mg L^{-1})				
	100	200	300	600	700
q_e exp (mg/g)	95.8	212.9	242.1	292.7	319.3
Pseudo-first-order					
q_e(mg/g)	95.8	212.9	237.1	287.8	313.2
K_1(1/min)	0.1281	0.1204	0.1154	0.1100	0.1184
R^2	0.9933	0.9925	0.9915	0.9898	0.9919
ARE	0.4455	0.4279	0.5271	0.5810	0.5250
Pseudo-second-order					
q_e(mg/g)	98.0	217.8	252.7	302.1	328.4
K_2(g/mg.min)	0.0024	0.0011	0.0007	0.0006	0.0006
R^2	0.9985	0.9983	0.9969	0.9960	0.9975
ARE	0.2243	0.2342	0.3053	0.3571	0.2909
Intra-Paticle					
k id	5.8762	6.0102	9.7688	12.0173	12.6263
C	45.73	147.03	135.13	161.01	181.01
R^2	0.9954	0.9930	0.9936	0.9940	0.9939
ARE	0.6540	0.5026	0.3961	0.3796	0.3915

$$\mathbf{q_t} = \frac{\mathbf{k_2 q_e^2 t}}{\left(1 + \mathbf{k_2 k_e t}\right)} \tag{9}$$

where q_t, q_e and t are as defined above, and k_2 (g mg^{-1} min^{-1}) is the rate constant for the kinetic model. This model assumes that the rate of sorption is controlled by the sharing of electrons between the sorbent and sorbate, i.e. a chemical process. The rate constant (k_2) and q_e calculated for this study, along with R^2, and ARE are summarized in Table 4. The non-linear plots of pseudo second-order of Hg (II) ions onto CEWP at concentrations of 100, 200, 300, 600 and 700 mg L^{-1} is shown in Fig. 9. The values of k_2, and q_e along with R^2, and ARE were summarized in Table 4, and show that the pseudo second order model correlated with the

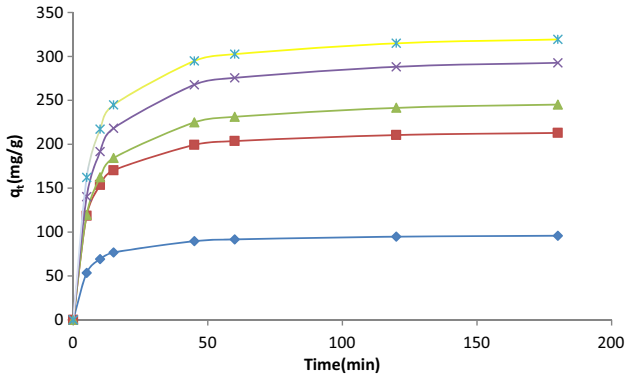

Fig. 9 Non-linear plots of pseudo-second-order models for adsorption of Hg (II) ions onto carbamoylethylatedwood pulp (CEWP) different concentrations (diamond 100 mg/L; square 200 mg/L; triangle 300 mg/L; cross 600 mg/L; star 700 mg/L).Reaction conditions: mercury acetate concentration: 300 mg/L; pH 5; contact time: 1 h; reaction temperature: 30 °C

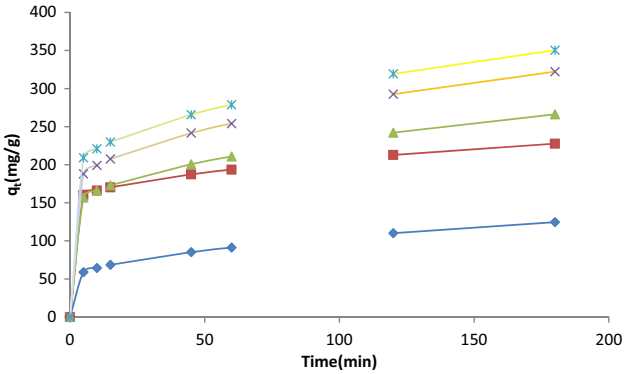

Fig. 10 Non-linear plots of intra-particle models for adsorption of Hg (II) ions onto carbamoylethylatedwood pulp (CEWP) different concentrations (diamond 100 mg/L; square 200 mg/L; triangle 300 mg/L; cross 600 mg/L; star 700 mg/L)..Reaction conditions: mercury acetate concentration: 300 mg/L; pH 5; contact time: 1 h; reaction temperature: 30 °C

experimental data with a minimum absolute residual error (ARE) and R^2 values compared to pseudo first order model for all concentrations in the range studied. This suggests that chemisorption is involved in the adsorption of Hg (II) onto CEWP [32]. The overall kinetics of sorption process, when controlled by intra-particle diffusion [33], can be expressed by:

$$q_t = k_{id}t^{0.5} + C \quad (10)$$

where q_t, and t are as defined above, and k_{id} (mg $g^{-1}min^{1/2}$) is the intra-particle diffusion rate constant. Previous studies report that a plot of q_t vs. $t^{1/2}$ gives multi-linear steps controlled by the sorption process [34, 35]. The initial portion is curved and due to bulk diffusion, followed by a linear portion attributed to intra-particle diffusion and, finally, a plateau, which results from equilibrium. The values of the C intercept (Table 4) give an idea about the boundary layer thickness, i.e. the intercept, the greater is the boundary layer effect [36]. The data of solid-phase metal concentration against time at the initial concentrations of 100, 200, 300, 600 and 700 mg L^{-1} were further processed for testing the rate of diffusion (as the rate-controlling step) in the sorption process. The sorption process studied here incorporates the transport of sorbate from the bulk solution to the interior surface of the pores in CEWP. It is possible that the transport of metal ions from the solution into the pores of the sorbent is the rate controlling step in batch experiments, especially with rapid stirring [37]. The rate parameter for intra-particle diffusion, k_p for five concentrations of Hg (II) are measured according to Eq. 10. The plots of q_t versus $t^{1/2}$ for the concentrations of 100, 200, 300, 600 and 700 mg L^{-1} are shown in Fig. 10. The values of k_p (mg g^{-1} min^{-1}) and are listed in Table 4. The results (Fig. 10) reveal a two-segment linear plot, indicating that the mechanism of sorption of Hg (II) on CEWP could be controlled by two or more steps [38, 39]. In the first segment, initial sorption begins with very rapid film diffusion, followed by slower intra-particle diffusion in the second stage, as the system approaches or attains equilibrium. The slope of the plot (Table 4) is a rate parameter, which is a characteristic of sorption where intra-particle diffusion is rate controlled. Also, the second segment deviates from the origin, which can be attributed to differences in the mass transfer rate between the initial and final sorption stages [40]. The absence of curvature in the plot indicates that there are no external mass transfer effects or boundary layer effects. Overall, the results obtained from the three kinetic models show that the sorption kinetic models can be ordered: pseudo-second-order > intra-particle > pseudo-first-order, for the quality of fit that they provide for the sorption of Hg (II) ions onto CEWP.

Mechanism of Sorption

The removal of Hg (II) ions from aqueous solution onto the surface of CEWP may occur via a combination of two mechanisms. Firstly, chelation occurs between the electron accepting Hg (II) ions and the nitrogen and oxygen electron

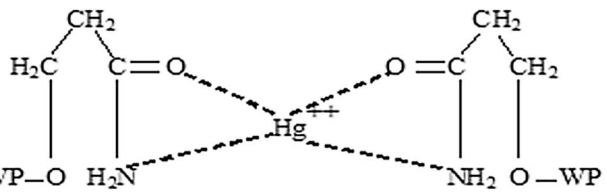

Scheme 1 Proposed complex structure between carbamoylethylated wood pulp (CEWP) and Hg (II) ions

donating groups present on the surface of CEWP, which are present as a result of the inherent chemistry and chemical transformations during the reaction (Scheme 1).

Secondly, intra-molecular dispersion occurs, comprising (a) movement of the sorbate from the bulk of the solution to the peripheral of the sorbent particle, (b) dispersion of the sorbate through the boundary layer to the external surface of the sorbent, (c) sorption at the dynamic sites on the external surface of CEWP, and (d) intra-particle-diffusion of the Hg (II) particles into the internal pores of the sorbent. This is supported by the kinetic fitting undertaken here, in tandem with the surface characterisation of the CEWP pre- and post-adsorption.

Conclusions

A new family of sorbents (CEWP) were prepared within this study, via carbamoylethylation of wood pulp (WP) with acrylamide in alkaline media. Morphological and chemical characteristics showed a clear modification of the base material with nitrogen functionalities and inherent oxygen containing moieties; the sorbent identified to have the highest level of modification was applied to the removal of Hg (II) ions from aqueous solutions. It was shown that the sorption capacity of CEWP was affected by sorbent dose, pH, contact time and metal ion concentration in solution and the results used to determine optimal conditions. The data obtained for sorption of Hg (II) ions on CEWP, under these optimised conditions, were analysed using a suite of two-parameter isotherm models (Langmuir, Freundlich, and Temkin), with the goodness of fit determined using non-linear regression. The analysis showed that the Temkin model provided the best fit of the experimental data, showing that surface heterogeneity influences this adsorption process, while the maximum sorption capacity according to Langmuir was 787.6 mg g^{-1}, at 30 °C, and sorption was deemed a favourable process via Freundlich analysis. The kinetics of sorption of Hg (II) onto CEWP were analysed using pseudo-first-order, pseudo-second-order, and intra-particle diffusion kinetic models, with the data described well by the pseudo-second-order model, suggesting overall chemical control of the sorption process, which may be controlled by a combination of physisorption, and complexation. Consequently, CEWP has been shown to be an effective sorbent for the removal of Hg (II) ions from aqueous solutions and demonstrates the potential role in water remediation processes.

References

1. Hashem A, Azzeer A, Ayoub A (2010) The Removal of Hg (II) Ions from Laboratory Wastewater onto Phosphorylated Haloxylon ammodendron: Kinetic and Equilibrium Studies. Polym-Plast Techno Eng 49(14):1463–1472
2. Mercury in Drinking-water in WHO Guidelines for Drinking-water Quality (GDWQ) 2005.
3. Peralta-Videa JR, Lopez ML, Narayan M, Saupe G (2009) The biochemistry of environmental heavy metal uptake by plants: implications for the food chain. Int J Biochem Cell Biol 41(8–9):1665–1677
4. Fu Y, Jiang J, Chen Z, Ying S, Wang J, Hu J (2019) Rapid and selective removal of Hg (II) ions and high catalytic performance of the spent adsorbent based on functionalized mesoporous silica/poly (m-aminothiophenol) nanocomposite. J Mol Liq 286:110746
5. Saman N, Kong H, Mohtar SS, Johari K, Mansor AF, Hassan O, Ali N, Mat H (2019) A comparative study on dynamic Hg (II) and MeHg (II) removal by functionalized agrowaste adsorbent: breakthrough analysis and adsorber design. Korean J Chem Eng 36(7):1069–1081
6. Tripathi A, Ranjan MR (2015) Heavy metal removal from wastewater using low cost adsorbents. J Bioremediation Biodegrad 6(06):1–5
7. Gunatilake S (2015) Methods of removing heavy metals from industrial wastewater. Methods 1(1):14
8. Abas SNA, Halim M, Ismail S, M. L. K, S. Izhar, (2013) Adsorption process of heavy metals by low-cost adsorbent: a review. World App Sci J 28(11):1518–1530
9. Di Natale F, Lancia A, Molino A, Di Natale M, Karatza D, Musmarra D (2006) Capture of mercury ions by natural and industrial materials. J Hazard Mater 132(2–3):220–225
10. Bethke K, Palantöken S, Andrei V, Roß M, Raghuwanshi VS, Kettemann F, Greis K, Ingber TTK, Stückrath JB, Valiyaveettil S (2018) Functionalized cellulose for water purification, antimicrobial applications, and sensors. Adv Funct Mat. 28(23):1800409
11. Chen X, Xu R, Xu Y, Hu H, Pan S, Pan H (2018) Natural adsorbent based on sawdust for removing impurities in waste lubricants. J Hazard Mater 350:38–45
12. Sirusbakht S, Vafajoo L, Soltani S, Habibi S (2018) Sawdust Bio sorption of Chromium (VI) Ions from Aqueous Solutions. Chem Eng Trans 70:1147–1152
13. Khalil MI, Moustafa Kh, Hebeish A (1993) Graft polymerization of acrylamide onto maize starch using potassium persulfate as initiator. Die Angewandte Makromolekulare Chemie 213:43–54
14. Tsai SC, Juang KW (2000) Comparison of Linear and Non-Linear Forms of Isotherm Models for Strontium Sor- ption on a Sodium Bentonite. Radioanalyt Nuclear Chem 243:741–746
15. Brunauer S, Emmett PH, Teller E (1938) Adsorption of gases in multimolecular layers. J Am Chem Society 60(2):309–319
16. Barrett EP, Joyner LG, Halenda PP (1951) The determination of pore volume and area distributions in porous substances I Computations from nitrogen isotherms. J Am Chem Society 73(1):373–380

17. Martín-Lara M, Hernainz F, Calero M, Blazquez G, Tenorio G (2009) Surface chemistry evaluation of some solid wastes from olive-oil industry used for lead removal from aqueous solutions. Biochem Eng J 44:151–159. https://doi.org/10.1016/j.bej.2008.11.012
18. Hashem A, Al-Anwar A, Nagy NM, Hussein DM, Eisa S (2016) Isotherms and kinetic studies on adsorption of Hg (II) ions onto Ziziphus spina-christi L from aqueous solutions. Green Processing Synthesis 5:213–224. https://doi.org/10.1515/gps-2015-0103
19. Chen H, Zhao Y, Wang A (2007) Removal of Cu(II) from aqueous solution by adsorption onto acid-activated palygorskite. J Hazard Mater 149:346–354
20. Khalil AA, Sokker HH, Al-Anwar A, Abd El-Zaher A, Hashem A (2009) Preparation, Characterization and Utilization of Amidoximated Poly (AN/MAA)-Grafted Alhagi Residues for the Removal of Zn (II) from Aqueous Solution. Adsorpt Sci Technol 27:363–382
21. Hashem A, Hussein HA, Sanousy MA, Adam E, Saad EE (2011) Monomethylolated thiourea–sawdust as a new adsorbent for removal of Hg (II) from contaminated water: equilibrium kinetic and thermodynamic studies. Polym-Plast Technol Eng 50:1220–1230
22. Langmuir I (1916) The constitution and fundamental properties of solids and liquids Part I Solids. J Am Chem Society. 38(11):2221–2295
23. Freundlich H (1907) Über die adsorption in lösungen. Zeitschrift für Physikalische Chemie 57(1):385–470
24. Temkin M (1940) Kinetics of ammonia synthesis on promoted iron catalysts. Acta Physiochimica URSS 12:327–356
25. Hashem A, Sanousy MA, Mohamed LA, Okoye PU, Hameed BH (2020) Natural and low-cost p turgidum for efficient adsorption of Hg (II) ions from contaminated solution: isotherms and kinetics studies. J Polym Enviro. https://doi.org/10.1007/s10924-020-01879-5
26. Hashem A, Fletcher AJ, El-Sakhawy M, Mohamed LA, Farag S (2020) Aminated hydroximoyl camelthorn residues as a novel adsorbent for extracting Hg (II) from contaminated water: Studies of Isotherm: Kinetics, and Mechanism. J Polym Enviro 28:2498–2510
27. Li B, Li M, Zhang J, Pan Y, Huang Z, Xiao H (2019) Adsorption of Hg (II) ions from aqueous solution by diethylenetriamine pentaacetic acid-modified cellulose. Int J Biol Macromol 122:149–156. https://doi.org/10.1016/j.ijbiomac.2018.10.162
28. Jiang J, Wang X (2019) Adsorption of Hg (II) ions from aqueous solution by thiosemicarbazide-modified cellulose adsorbent. BioResources 14:4670–4695
29. Ding Z, Yu R, Hu X, Chen Y (2014) Adsorptive removal of Hg (II) ions from aqueous solutions using chemical-modified peanut hull powder. Polish J Enviro Studies. 23:1115–1121
30. Lagergren SK (1898) About the theory of so-called adsorption of soluble substances. Sven Vetenskapsakad Handingarl 24:1–39
31. Ho Y-S, McKay G (1999) Pseudo-second order model for sorption processes. Process Biochem 34(5):451–465
32. LR Somera R Cuazon J.K., Cruz L, J. Diaz, 2019 Kinetics and Isotherms Studies of the Adsorption of Hg (II) onto Iron Modified Montmorillonite/Polycaprolactone Nanofiber Membrane IOP Conference Series: Materials Science and Engineering. 540 1 012005
33. Weber WJ, Morris JC (1963) Kinetics of adsorption on carbon from solution. J Sanit Eng Div 89(2):31–60
34. Boparai HK, Joseph M, O'Carroll DM (2011) Kinetics and thermodynamics of cadmium ion removal by adsorption onto nano zerovalent iron particles. J Hazard Mater 186(1):458–465
35. Unuabonah E, Adebowale K, Olu-Owolabi B (2007) Kinetic and thermodynamic studies of the adsorption of lead (II) ions onto phosphate-modified kaolinite clay. J Hazard Mater 144(1–2):386–395
36. Kannan N, Sundaram MM (2001) Kinetics and mechanism of removal of methylene blue by adsorption on various carbons—a comparative study. Dyes Pigm 51(1):25–40
37. Poots V, McKay G, Healy J (1978) Removal of basic dye from effluent using wood as an adsorbent. J Water Pollut Control Fed 50:926–935
38. Marrakchi F, Ahmed MJ, Khanday WA, Asif M, Hameed BH (2017) Mesoporous-activated carbon prepared from chitosan flakes via single-step sodium hydroxide activation for the adsorption of methylene blue. Int J Biol Macromol 98:233–239
39. Kołodynska D, Hałas P, Franus M, Hubicki Z (2017) Zeolite properties improvement by chitosan modification—Sorption studies. J Ind Eng Chem 52:187–196
40. Tsibranska I, Hristova E (2011) Comparison of different kinetic models for adsorption of heavy metals onto activated carbon from apricot stones. Bul Chem Commun 43:370